Original Article

Increase in GPIHBP1 expression in advanced stage colorectal cancer indicates poor immune surveillance

Min Gao[1#], Liting Liao[1#], Zhijie Lin[1,2^], Xiangyu Hu[1,2], Linhui Jia[1,2], Weijuan Gong[1,2,3,4,5^], Xiaoqin Jia[1,2,3,4,5]

[1]Department of Pathobiology, School of Medicine, Yangzhou University, Yangzhou, China; [2]Department of Gastroenterology, Affiliated Hospital, Yangzhou University, Yangzhou, China; [3]Department of General Surgery, Affiliated Hospital, Yangzhou University, Yangzhou, China; [4]Jiangsu Key Laboratory of Integrated Traditional Chinese and Western Medicine for Prevention and Treatment of Senile Diseases, Yangzhou, China; [5]Jiangsu Key Laboratory of Zoonosis, Yangzhou, China

Contributions: (I) Conception and design: W Gong, X Jia; (II) Administrative support: W Gong, X Jia; (III) Provision of study materials or patients: W Gong, X Jia; (IV) Collection and assembly of data: M Gao, L Liao, X Hu, L Jia; (V) Data analysis and interpretation: M Gao, L Liao, X Hu, L Jia, Z Lin; (VI) Manuscript writing: All authors; (VII) Final approval of manuscript: All authors.

[#]These authors contributed equally to this work as co-first authors.

Correspondence to: Xiaoqin Jia, PhD. Department of Pathobiology, School of Medicine, Yangzhou University, 136 Jiangyang Rd., Yangzhou 225001, China; Department of Gastroenterology, Affiliated Hospital, Yangzhou University, Yangzhou 225001, China; Department of General Surgery, Affiliated Hospital, Yangzhou University, Yangzhou 225001, China; Jiangsu Key Laboratory of Integrated Traditional Chinese and Western Medicine for Prevention and Treatment of Senile Diseases, Yangzhou 225001, China; Jiangsu Key Laboratory of Zoonosis, Yangzhou 225001, China. Email: xqjia@yzu.edu.cn.

Background: Glycosylphosphatidylinositol (GPI)-anchored high-density lipoprotein-binding protein 1 (GPIHBP1) plays a crucial role in fatty acid metabolism, which is involved in the progression of colorectal cancer (CRC). The aim of this study was to determine the expressional variations of GPIHBP1 in CRC at different stages and to verify whether this protein affects the shaping of the immune microenvironment of cancer cells.

Methods: Variations of GPIHBP1 messenger RNA (mRNA) levels were first analysed using The Cancer Genome Atlas (TCGA) database. Protein levels of GPIHBP1 in cancer nest cells, stromal cells or surrounding normal tissues from 68 patients with CRC were checked by immunohistochemistry. Infiltration of immune cells such as macrophages, myeloid-derived suppressor cells (MDSCs), $CD8^+$ and $CD56^+$ cells was parallelly stained in the same tissues. Ectopic GPIHBP1 expressed colonic tumour cells were transplanted into the back of mice. Tumour growth and immune cell infiltrations were also observed.

Results: Compared with those in healthy tissues, GPIHBP1 mRNA and protein levels decreased in the patients with CRC at Dukes A–B stage but gradually increased in the patients at Dukes C–D stage. GPIHBP1 in foci or stroma was positively correlated with recruited macrophages or MDSCs and negatively correlated with recruited $CD8^+$, $CD56^+$ or granzyme$^+$ cells. The mice injected with GPIHBP1 overexpression cells bore large tumours. Histological analysis confirmed the infiltration of many macrophages and MDSCs but less $CD8^+$ T or $CD56^+$ cells.

Conclusions: The increased expression of GPIHBP1 is involved in the progression of CRC. High GPIHBP1 level of advanced CRC indicates efficient immune evasion in tumour microenvironment.

Keywords: Glycosylphosphatidylinositol-anchored high-density lipoprotein-binding protein 1 (GPIHBP1); expression; colorectal cancer (CRC); immune surveillance

^ ORCID: Zhijie Lin, 0000-0001-6890-1225; Weijuan Gong, 0000-0002-8543-1314.

Submitted Sep 23, 2023. Accepted for publication May 08, 2024. Published online Jun 11, 2024.
doi: 10.21037/tcr-23-1766
View this article at: https://dx.doi.org/10.21037/tcr-23-1766

Introduction

Glycosylphosphatidylinositol (GPI)-anchored high-density lipoprotein-binding protein 1 (GPIHBP1) is mainly located on the luminal surface of capillary endothelial cells and is a member of a large family of GPI-anchored lymphocyte antigen 6 (Ly6) proteins. GPIHBP1 has four domains: a signal peptide, an amino-terminal acidic domain, a cysteine-rich Ly6 domain and a GPI-linked hydrophobic carboxyl-terminal domain. The acidic and Ly6 domains of GPIHBP1 co-ordinately bind lipoprotein lipase (LPL) to hydrolyse lipoprotein triglycerides, releasing nutrients to surrounding tissues (1,2). *Gpihbp1*-deficient mice exhibit milky plasma and plasma triglyceride levels of 2,500–5,000 mg/dL even under a chow diet (3). The mutation of GPIHBP1 results in severe hypertriglyceridemia and pancreatitis. Similarly, the GPIHBP1 autoantibody syndrome is also associated with severe hypertriglyceridemia and recurrent episodes of acute pancreatitis (4,5). Whether GPIHBP1 expression affects tumour progression remains unknown.

Tumour development depends on the reprogramming of cell metabolism (6,7). Tumour cells can obtain essential nutrients from nutrient-deficient environment and use these nutrients to maintain their viability. Changes in the intracellular and extracellular metabolites of tumour cells can have profound effects on gene expression, cell differentiation and shaping microenvironment (8,9). Compared with normal tissues, tumours exhibit remarkably increased consumption of glucose (10) and glutamine (11) *in situ*. Tumour cells in blood or lymph vessels need to overcome anoikis and thus mainly use pyruvate to produce additional nicotinamide adenine dinucleotide phosphate (NADPH) as energy supply (12). Nevertheless, metastatic tumour cells require a large amount of adenosine triphosphate (ATP) for transendothelial movement and colonisation into distant organs and thus mainly depend on energy from mitochondrial oxidative phosphorylation (12). Cancer metastasis usually involves the enhancement of fatty acid metabolism (13). Multiple metastatic tumours up-regulate the expression of CD36 and fatty acid-binding proteins and utilise fatty acid oxidative phosphorylation for energy supply (14,15).

GPIHBP1 plays a vital role in the lipolytic process and has been identified as responsible for transporting LPL into capillaries, which is crucial for triglyceride metabolism (1). Moreover, patients with colorectal cancer (CRC) exhibit up-regulation of lactic acid and plasma lipids (16), suggesting the involvement of fatty acid metabolism in CRC progression. The objective of this study was to explore variations of GPIHBP1 expression levels across different stages of CRC and analyse the potential impact of GPIHBP1 levels on the immune microenvironment. We present this article in accordance with the ARRIVE reporting checklist (available at https://tcr.amegroups.com/article/view/10.21037/tcr-23-1766/rc).

Highlight box

Key findings

- The increased expression of glycosylphosphatidylinositol-anchored high-density lipoprotein-binding protein 1 (GPIHBP1) is involved in the progression of colorectal cancer (CRC). High GPIHBP1 level of advanced CRC indicates efficient immune evasion in tumour microenvironment.

What is known and what is new?

- GPIHBP1 plays a vital role in the lipolytic process and has been identified as responsible for transporting lipoprotein lipase into capillaries, which is crucial for triglyceride metabolism.
- This study firstly presented that tumour cells themselves could upregulate GPIHBP1 expression to facilitate immune evasion.

What is the implication, and what should change now?

- Suppression of GPIHBP1 expression would theoretically repress the progression of CRC in patients with advanced CRC.

Methods

Animals and cell lines

Specific pathogen-free C57BL/6J wild-type mice were provided by the Comparative Medical Center of Yangzhou University. All animals used in this study were females, 8–10 weeks old. All animal experiments were reviewed and approved by the Institutional Animal Care and Use Committee of Yangzhou University (No. YXYLL-2022-56), in compliance with institutional guidelines for the care and use of animals. A protocol was prepared before the

study without registration. Human embryonic kidney cells 293T, mouse colon adenocarcinoma cells MC38, CT26 and CMT93, mouse liver cancer cells H22 were acquired from the American Type Culture Collection. All cell lines were maintained in Dulbecco's modified Eagle's medium (DMEM) supplemented with 10% fetal bovine serum (FBS), streptomycin and penicillin. GPIHBP1 ORF DNA (NM_026730.2) was cloned and inserted into a pLVX-acGFP1 lentiviral expression vector. Lentiviruses were packaged with vector pLP1, pLP2, and pLP/VSVG in 293T cells by Lipofectamine 3000 Reagent (ThermoFisher Scientific, Waltham, MA, USA). MC38 cells were infected with lentiviruses (GPIHBP1 or Mock vector) together with polybrene (10 μg/mL). Stable GPIHBP1-expressing cells were obtained through puromycin selection.

Bioinformatics

Data on the variations of GPIHBP1 in CRC, including immune cell infiltration, gene expression (level 3 HTSeq-FPKM) and related clinical information (comprising 51 normal and 647 tumour samples) were obtained from The Cancer Genome Atlas (TCGA) database (17). Patients with CRC (n=647) were divided into two groups according to GPIHBP1 expression. GPIHBP1 (ENSG00000277494) messenger RNA (mRNA) data and related clinical information were processed on R language (version 3.6.3). tumour-node-metastasis (TNM) stage was classified following the 8th edition [2017] TNM Classification for CRC of the American Joint Committee on Cancer. Kaplan-Meier survival analysis was performed to analyse the relationship between the expression of GPIHBP1 and the survival status of patients with CRC. The correlation between GPIHBP1 expression and markers of neutrophils or macrophages described previously (18) was validated using gene set variation analysis (19). The study was conducted in accordance with the Declaration of Helsinki (as revised in 2013). This research involving human participants was reviewed and approved by the Ethics Committee of the Affiliated Hospital of Yangzhou University (No. 2021-YKL4-28-004). All patients signed informed consent forms.

Patients and tumour samples

Tumour surgical samples were collected from 68 patients with CRC (43 males and 25 females) aged 31–82 years with an average of 62.7 years. Para-cancerous tissues which were 5 cm away from the edge of primary tumours were stored as the control. All tumour tissues were identified as adenocarcinoma by two independent pathologists. Clinical features of these patients are shown in Table S1.

Reagents and antibodies

The following antibodies were used for flow cytometry and obtained from ThermoFisher Scientific: CD3-APC/Cy7 (145-2C11) and CD11b-APC/Cy7 (M1/70); BioLegend (San Diego, CA, USA): NK1.1-APC (PK136), CD4-PE (GK1.5), CD8a-PE (53-6.7), F4/80-PE (BM8), F4/80-FITC (BM8), CD206-FITC (C068C2), CD86-PE (GL-1), CD11c-PE/Cy7 (N418), and Gr-1-PE (RB6-8C5); BD Pharmingen (San Diego, CA, USA): F4/80-APC (T45-2342) and CD8a-PE/Cy7 (53-6.7). The specific immune cells were visualized using flow markers. $CD8^+$ T cell: $CD3^+CD8a^+$; natural killer (NK) cell: $CD3^-NK1.1^+$; $CD4^+$ T cell: $CD3^+CD4^+$; macrophage: $CD11b^+F4/80^+$; M1 macrophage: $CD11b^+F4/80^+CD86^+$; M2 macrophage: $CD11b^+F4/80^+CD206^+$; myeloid-derived suppressor cell (MDSC): $CD11b^+Gr\text{-}1^+$. A lentivirus vector system was purchased from GENECHEM Company (Shanghai, China). The following antibodies were used for immunohistochemistry: GPIHBP1 antibody from Abcam (ab224725; Cambridge, UK); F4/80 (70076S) and CD56 (99746S) from Cell Signalling Technology (Danvers, MA, USA); CD68 (macrophage marker; 66231-2-IG), CD8 (66868-1-IG), arginase 1 (Arg1; M2 macrophage marker; 66129-1-IG) (20), and S100A8 (MDSCs marker, 15792-1-AP) (21) from Proteintech (Wuhan, China); and antibody (MA5-17139) against inducible nitric oxide synthase (iNOS; M1 macrophage marker) (20) from ThermoFisher Scientific; granzyme B (GZMB) antibody (NBP2-76414) from Novus Biologicals (Littleton, CO, USA).

Immunohistochemistry

All tumour samples were fixed in 10% neutral buffer formalin overnight. Tumour sections (5 μm) were dehydrated with ethanol and embedded in paraffin. After hydrogen peroxide (3%) and sodium citrate (10 mM, pH 6, 95 ℃ supplied by a microwave oven) were sequentially used to block cell-intrinsic peroxidase activity and repair antigen in colorectal sections, bovine serum albumin (BSA; 5%) was used to block the sections. The sections were then incubated with primary antibody overnight in a refrigerator shaker at 4 ℃ and stained with peroxidase-conjugated secondary antibody [goat anti-rabbit or anti-

mouse immunoglobulin G (IgG), Invitrogen, Carlsbad, CA, USA]. After being added with substrate (diaminobenzidine tertrahydrochloride, Cowin Biotech, Beijing, China) and re-stained by haematoxylin (Servicebio, Beijing, China), the colour of the sections was observed under a high-power optical microscope.

Semi-quantitative analysis of staining results

Five visual fields were randomly selected for each section and examined under a high-power microscope. The number of positive cells per 1,000 tumour cells was calculated. The histological evaluation of GPIHBP1 was conducted separately in tumour foci and stroma. The expression of CD68, CD56, CD8, Arg1, iNOS, S100A8, and GZMB in the tumour stroma was also assessed. The percentage of positive cells was categorized as follows: <5%, 0; 5–20%, 1; 20–40%, 2; 40–60%, 3; 60–80%, 4; 80–90%, 5; and 90–100%, 6. The criteria for staining intensity were as follows: 0 for cells that were not stained or had a colour similar to the background, 2 for cells with a slightly lighter or darker colour than the background, 4 for cells with a moderate colour or protruding from the background, and 6 for cells with strong brown staining. The final score for each tissue sample was the sum of the two scores: (–) for scores ranging from 0 to 3, (+) for scores ranging from 4 to 6, (++) for scores ranging from 7 to 9, and (+++) for scores ranging from 10 to 12. The pathological results were independently assessed by two senior pathologists, and a third senior physician randomly checked the objectivity and accuracy of the pathological scores.

Transplanted tumours

GPIHBP1 overexpressing cell lines MC38-GPIHBP1 or CT26-GPIHBP1 in logarithmic phase were subcutaneously injected into C57B/L6 or BALB/c mice respectively (1.5×10^6 cells in 200 µL phosphate buffer solution per mouse). The growth of transplanted tumour was observed every day, and the volume was calculated (volume = length × width^2/2). On the 19th day, all mice were sacrificed and tumour tissues were separated. The weight of transplanted tumours was measured *ex vitro*.

Isolation of mononuclear cells

Tumour-infiltrating immune cells were isolated using density-gradient centrifugation (22). Briefly, tumour tissues were cut into small pieces (0.5–1.0 mm) using scissors. Then, the tissues were meshed through the cell strainer (70 µm) using the rubber plunger of a syringe. The immune cells were isolated by density-gradient centrifugation with 30% Percoll solution.

Western blot

Cell lysates were extracted and protein concentration was measured using NanoDrop. Equal amounts of protein (20 µg) were separated by 15% sodium dodecyl sulfate-polyacrylamide gel electrophoresis (SDS-PAGE) and transferred to polyvinylidene fluoride membranes; nonspecific sites were blocked with 5% BSA in tris-buffered saline with Tween-20 (TBST) and the membranes were then incubated with anti-GPIHBP1 (1:1,000; Abcam; ab224728), ACC (1:1,000; Cell Signalling Technology; 3676), p-ACC (1:1,000; Cell Signalling Technology; 3661), CPT-1α (1:1,000; Proteintech; 66039-1-Ig), C/EBPβ (1:1,000; Abcam; ab53138), Glut1 (1:1,000; Proteintech; 66290-1-Ig) and anti-β-actin (1:5,000; Servicebio; GB15001); were sequentially incubated with horse radish peroxidase conjugated anti-rabbit or anti-mouse secondary antibody (1:2,000; Invitrogen). Western blots were visualized using the enhanced chemiluminescence kit (Vazyme, Beijing, China).

Flow cytometry

Immune cells were stained with corresponding antibodies at 4 ℃ for 30 min, and detected by BD FACSVerse system. All data were analysed by FlowJo software (version 10.4; FlowJo LLC, Franklin Lakes, NJ, USA).

Statistical analysis

Continuous variables were presented as mean ± standard deviation using GraphPad Prism 9.0 (GraphPad Software, San Diego, CA, USA). The Student's *t*-test was utilized to compare the difference between the two groups of data. Analysis of variance (ANOVA) was applied for multiple comparisons of data, and P values were adjusted using Tukey's method. The Shapiro-Wilk test was used to assess the normality of the data, and if the data did not follow a normal distribution, the Wilcoxon rank sum test was chosen. Spearman correlation coefficient was utilized for linear correlation analysis. All analyses were carried out using SPSS 18.0 (IBM, Armonk, NY, USA). Significance of difference was indicated by P<0.05 (*), P<0.01 (**), and

P<0.001 (***).

Results

Variations of GPIHBP1 in CRC according to in silico analysis

According to the TCGA database, the transcription of GPIHBP1 remarkably decreased in patients with CRC (n=647) compared with that in healthy controls (n=51) (*Figure 1A*). GPIHBP1 transcription of tumour tissues also decreased compared with that in the surrounding normal tissue within the same individual (*Figure 1B*). Patients with CRC showing a high level of GPIHBP1 had poor life expectancy (*Figure 1C*). Unexpectedly, GPIHBP1 transcription decreased in the early stage (T1/T2) of CRC but was relatively elevated in the late stage (T3, T4, or N2) (*Figure 1D*).

The tumour-infiltrating immune cells have a significant association with the prediction of overall survival in CRC. Analysis from the TCGA database revealed that neutrophils and macrophages were significantly enriched in GPIHBP1^{high}-tumours compared to GPIHBP1^{low}-tumours (*Figure 1E*). In summary, the expression of GPIHBP1 in CRC tissues was found to be decreased at the early stage and increased at the late stage. This variation in expression might have an influence on local immune cell infiltration.

GPIHBP1 expression in patients with CRC as revealed by immunohistochemistry

The tumour samples of patients with CRC (n=68) were collected to check the protein level changes of GPIHBP1. In line with the transcriptional variation, the staining of GPIHBP1 on CRC sections substantially decreased in the early stage (Dukes A/B) but increased in the late stage and was particularly enhanced in the tumour foci (Dukes C/D (*Figure 2A*). The GPIHBP1 expression in tumour cell nests or stroma of tumour tissues was then analysed.

The low GPIHBP1 expression in the early stage and its high expression in the late stage only occurred in the tumour cells. In the stroma of CRC, GPIHBP1 expression was gradually up-regulated with disease progression (*Figure 2B-2D*). Thus, the expression of GPIHBP1 in the carcinoma cells of patients with CRC was confirmed to progressively increase. Additionally, it was observed that the stromal cells also exhibited an increasing expression of GPIHBP1 with CRC progression.

Association of GPIHBP1 level with the infiltration of myeloid cells in patients with CRC

The expression levels of CD68, Arg1, iNOS, and S100A8 were also parallelly checked in the tumour samples of patients with CRC. The staining of CD68, Arg1, and S100A8 increased in the advanced stages, and no change was observed for iNOS (*Figure 3A*,*3B*). The GPIHBP1 expression level in tumour foci was positively correlated with the staining score (based on staining intensities and numbers) of CD68, Arg1, and S100A8, but was not correlated with that of iNOS (*Figure 3C*). Furthermore, the GPIHBP1 expression level of stromal cells was strongly correlated with the staining score of CD68, Arg1, and S100A8, but had no correlation with that of iNOS (*Figure 3D*). These results indicated that the increased GPIHBP1 expression in CRC was associated with the recruitment of tumour-promoting myeloid cells (such as M2 macrophages and MDSCs).

Association of GPIHBP1 level with CD8$^+$ or CD56$^+$ cells in patients with CRC

The infiltration of cytotoxic immune cells such as CD8$^+$ T or CD56$^+$ cells in the patients with CRC was investigated. The number of CD8$^+$, CD56$^+$, and GZMB$^+$ cells decreased as the disease progressed (*Figure 4A*,*4B*). Meanwhile, the elevated expression of GPIHBP1 either in cancer nest cells (*Figure 4C*) or stromal cells (*Figure 4D*) was negatively correlated with staining score of CD8$^+$, CD56$^+$, or GZMB$^+$ cells. Thus, the high GPIHBP1 expression in CRC indicated poor immune surveillance.

Ectopic expression of GPIHBP1 promoted tumour growth and increased infiltration of immune-suppressive cells

The expression of GPIHBP1 was confirmed to be present in 293T and CMT93 cells, but only minimally expressed in MC38 and H22 cells (*Figure 5A*). Thus, MC38 cells with the ectopic GPIHBP1 expression (MC38-GPIHBP1) were generated *in vitro* (*Figure 5B*, Figure S1A). We conducted an examination of the key proteins involved in glycolipid metabolism in cells that overexpress GPIHBP1. We observed an upregulation in the levels of p-ACC and CPT1α. However, we also noticed a downregulation in the expression of Glut1 (*Figure 5C*). These findings suggest that overexpression of GPIHBP1 might promote fatty acid oxidation in CRC cells.

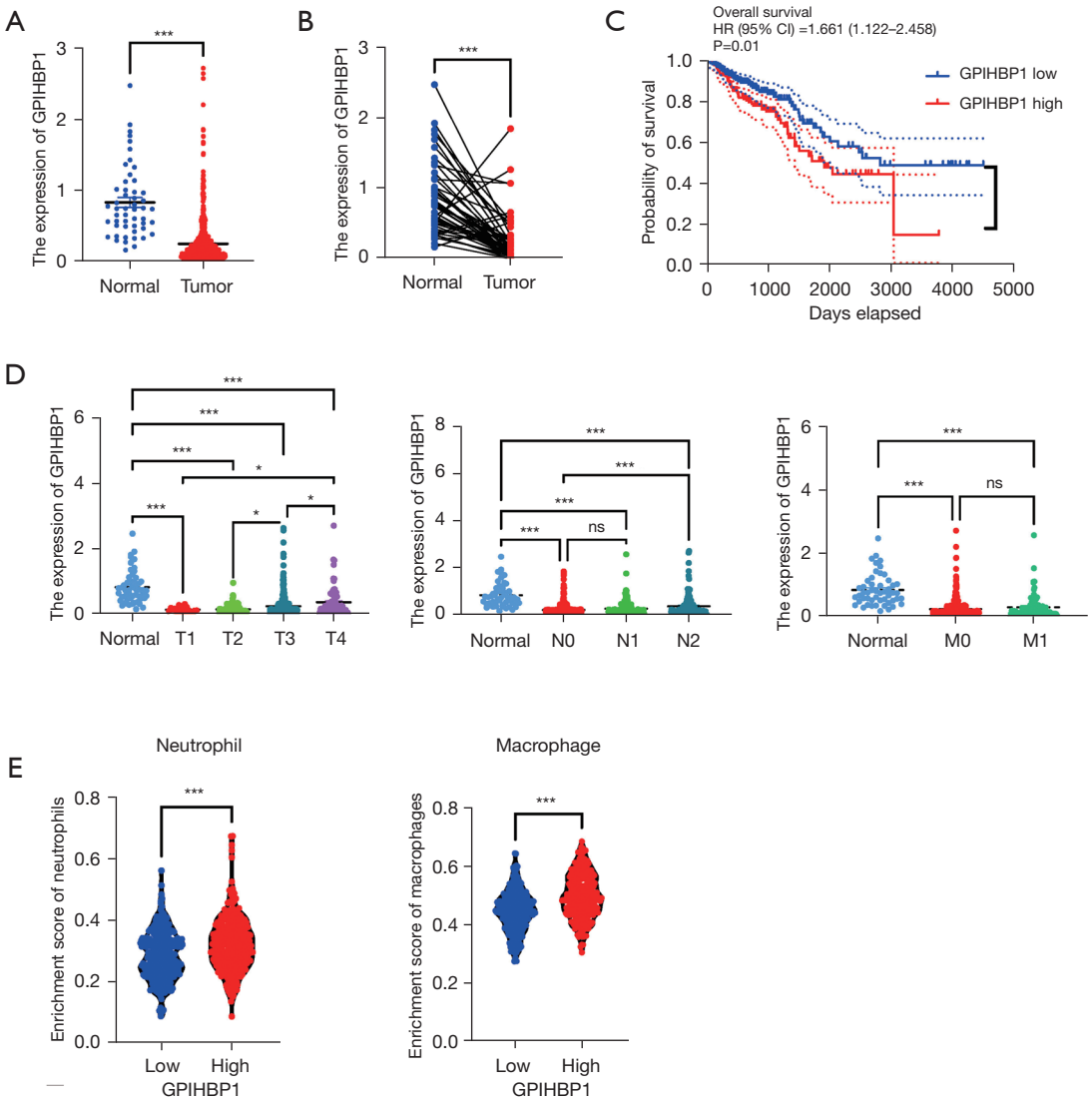

Figure 1 Bioinformatics of GPIHBP1 mRNA in CRC based on TCGA data. (A) The expression of GPIHBP1 mRNA in healthy control and CRC samples. (B) The expression of GPIHBP1 mRNA in tumour tissues and surrounding normal tissues. (C) Survival analysis of GPIHBP1^{high} and GPIHBP1^{low} patients, data are presented as HR (95% CI). (D) Variations of GPIHBP1 mRNA in CRC patients of different TNM stages. (E) Enrichment scores of neutrophils and macrophages in GPIHBP1^{high} and GPIHBP1^{low} patients. ns, no significance; *, P<0.05; ***, P<0.001. GPIHBP1, GPI-anchored high-density lipoprotein-binding protein 1; GPI, glycosylphosphatidylinositol; HR, hazard ratio; CI, confidence interval; mRNA, messenger RNA; CRC, colorectal cancer; TCGA, The Cancer Genome Atlas; TNM, tumour-node-metastasis.

When MC38-Mock or MC38-GPIHBP1 cells were subcutaneously injected into the back of mice, large tumours were observed in the mice with MC38-GPIHBP1 cells (*Figure 5D-5F*). Meanwhile, the CD8$^+$ T, NK, or CD4$^+$ T, cells remarkably decreased in the single cell suspension of tumours analysed in flow cytometry, but the macrophages (CD11b$^+$F4/80$^+$) and MDSCs (CD11b$^+$Gr-1$^+$) increased (*Figure 5G*, Figure S1B-S1I) in the mice injected with MC38-GPIHBP1 cells. No changes of dendritic cells were found in the tumour tissues (Figure S1J). The decrease in F4/80$^+$CD86$^+$ cells and the increase in F4/80$^+$CD206$^+$ cells in the MC38-GPIHBP1-transplanted mice (*Figure 5G*) indicated the intensified M2 macrophage polarisation in the tumour microenvironment. These findings were verified in

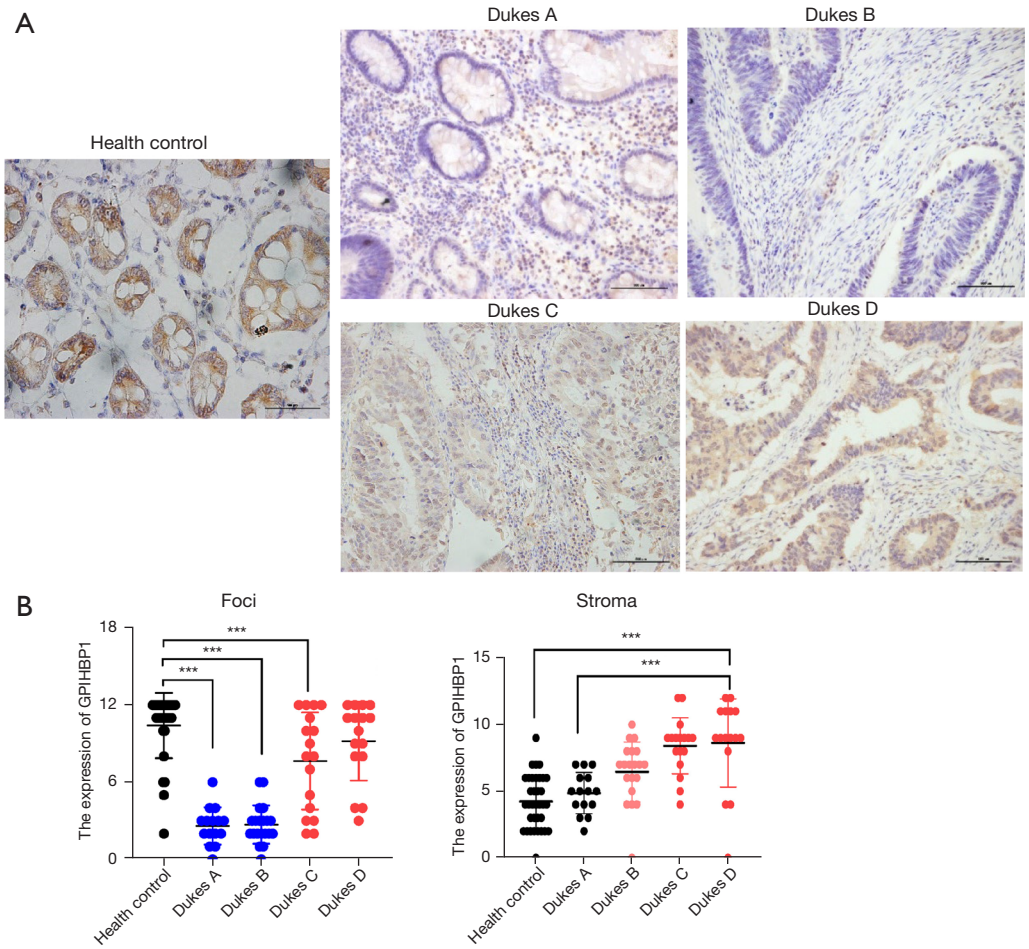

C

CRC stage	GPIHBP1 in foci				SUM	Rs	P
	–	+	++	+++			
Health control	13	20	6	29	68		
Dukes A	12	3	0	0	15		
Dukes B	16	4	0	0	20	0.702	<0.01
Dukes C	4	2	4	7	17		
Dukes D	1	2	4	9	16		

D

CRC stage	GPIHBP1 in stroma				SUM	Rs	P
	–	+	++	+++			
Health control	14	36	17	1	68		
Dukes A	3	9	3	0	15		
Dukes B	1	7	11	1	20	0.51	<0.01
Dukes C	0	3	11	3	17		
Dukes D	1	2	7	6	16		

Figure 2 Variations of GPIHBP1 protein levels in CRC. (A) IHC staining results of GPIHBP1 in patients with different stages of CRC (scale bar: 50 μm). (B) Comparison of GPIHBP1 presence in cancer foci or stroma. (C,D) Correlational study of GPIHBP1 presence in cancer foci or stroma with CRC progression. ***, P<0.001. GPIHBP1, GPI-anchored high-density lipoprotein-binding protein 1; GPI, glycosylphosphatidylinositol; CRC, colorectal cancer; IHC, immunohistochemistry.

the GPIHBP1-overexpressed CT26 cell line (Figure S2A). Large tumours were observed in the mice injected with CT26-GPIHBP1 cells (Figure S2B). The immune infiltration in CT26-GPIHBP1 tumour-bearing mice was similar to that observed in mice with MC38-GPIHBP1 tumours (Figure S2C-S2G). Histological analysis also confirmed the strong staining of F4/80, S100A8, and Arg1 and the minimal presence of $CD8^+$ cells in the tumours formed by MC38-GPIHBP1 cells. No changes of iNOS were observed in the two groups of tumours (*Figure 5H,5I*).

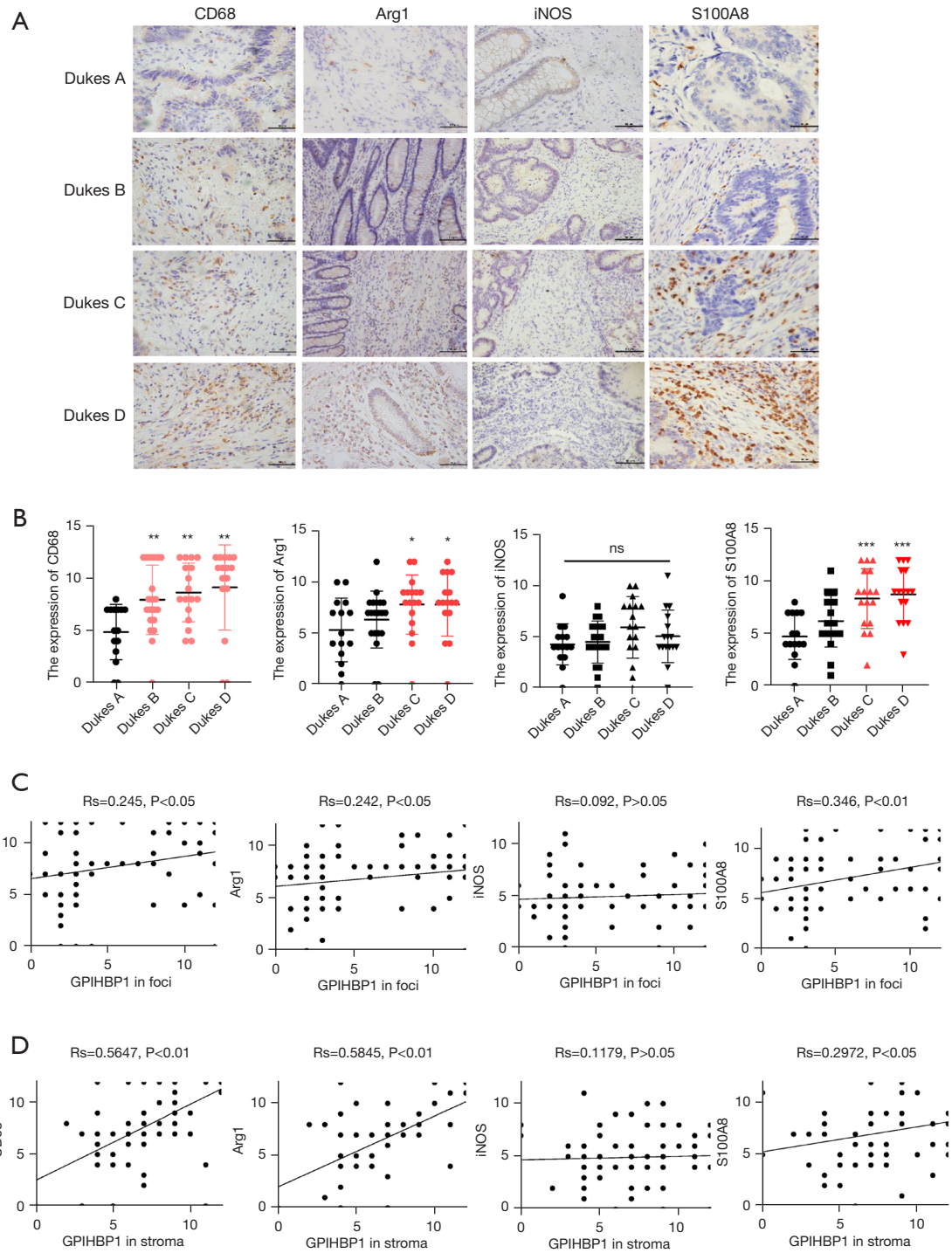

Figure 3 Macrophages and MDSCs in different stages of CRC. (A) Representative IHC staining results of CD68, Arg1, iNOS, and S100A8 (scale bar: 50 μm). (B) Comparisons of CD68, Arg1, iNOS, or S100A8 presence in patients with different stages of CRC. Correlational study of GPIHBP1 presence in cancer foci (C) or stroma (D) with above myeloid cell markers. ns, no significance; *, P <0.05; **, P<0.01; ***, P<0.001. Arg1, arginase 1; iNOS, inducible nitric oxide synthase; GPIHBP1, GPI-anchored high-density lipoprotein-binding protein 1; GPI, glycosylphosphatidylinositol; MDSC, myeloid-derived suppressor cell; CRC, colorectal cancer; IHC, immunohistochemistry.

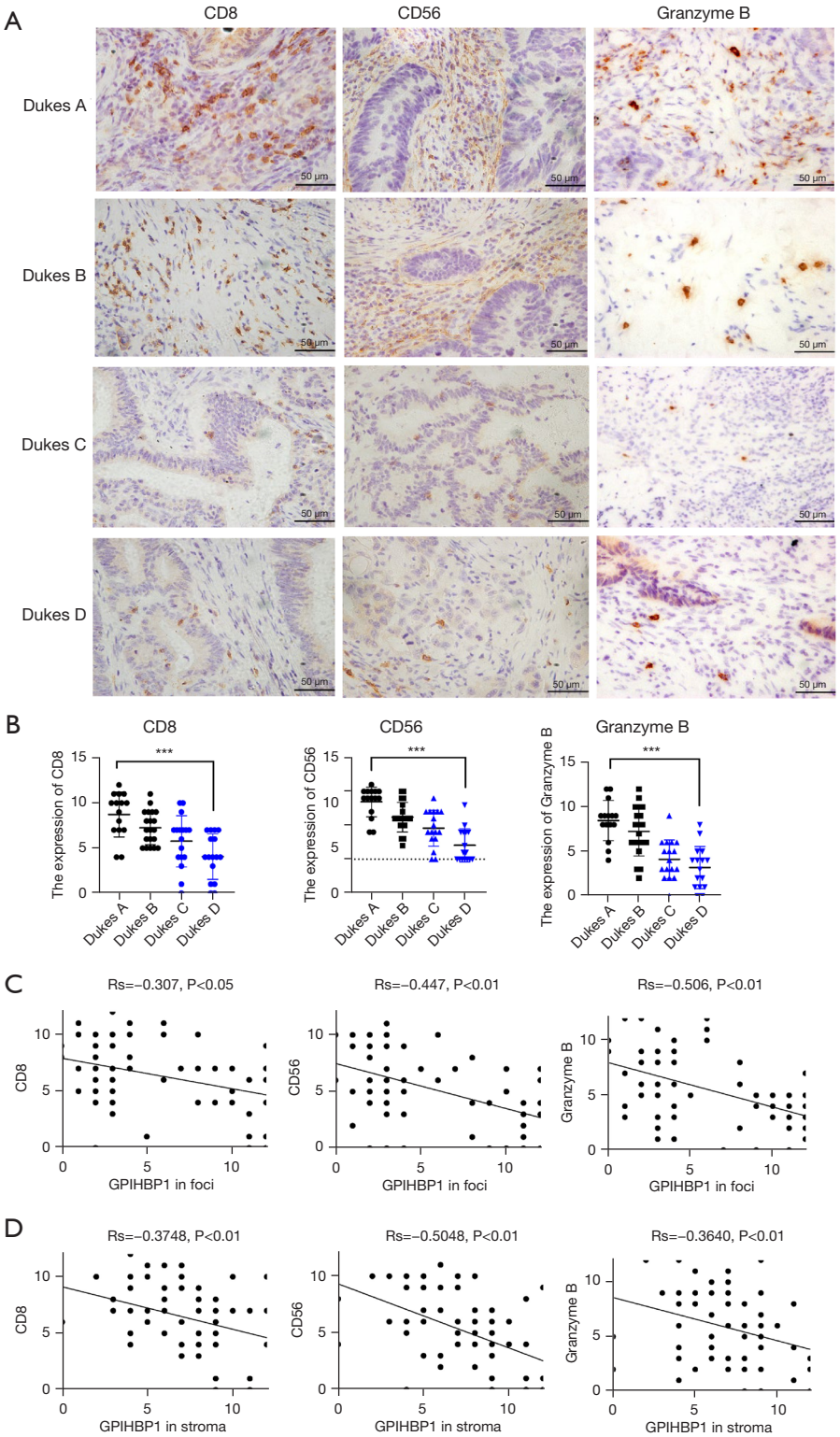

Figure 4 CD8$^+$ or CD56$^+$ cells infiltrated in CRC. (A) IHC staining results of CD8, CD56, and GZMB (scale bar: 50 μm). (B) Comparisons of CD8, CD56, or GZMB presence in patients with different stages of CRC. Correlational study of GPIHBP1 presence in cancer foci (C) or stroma (D) with infiltrations of CD8$^+$, CD56$^+$, and GZMB$^+$ cells. ***, P<0.001. GPIHBP1, GPI-anchored high-density lipoprotein-binding protein 1; GPI, glycosylphosphatidylinositol; CRC, colorectal cancer; IHC, immunohistochemistry; GZMB, granzyme B.

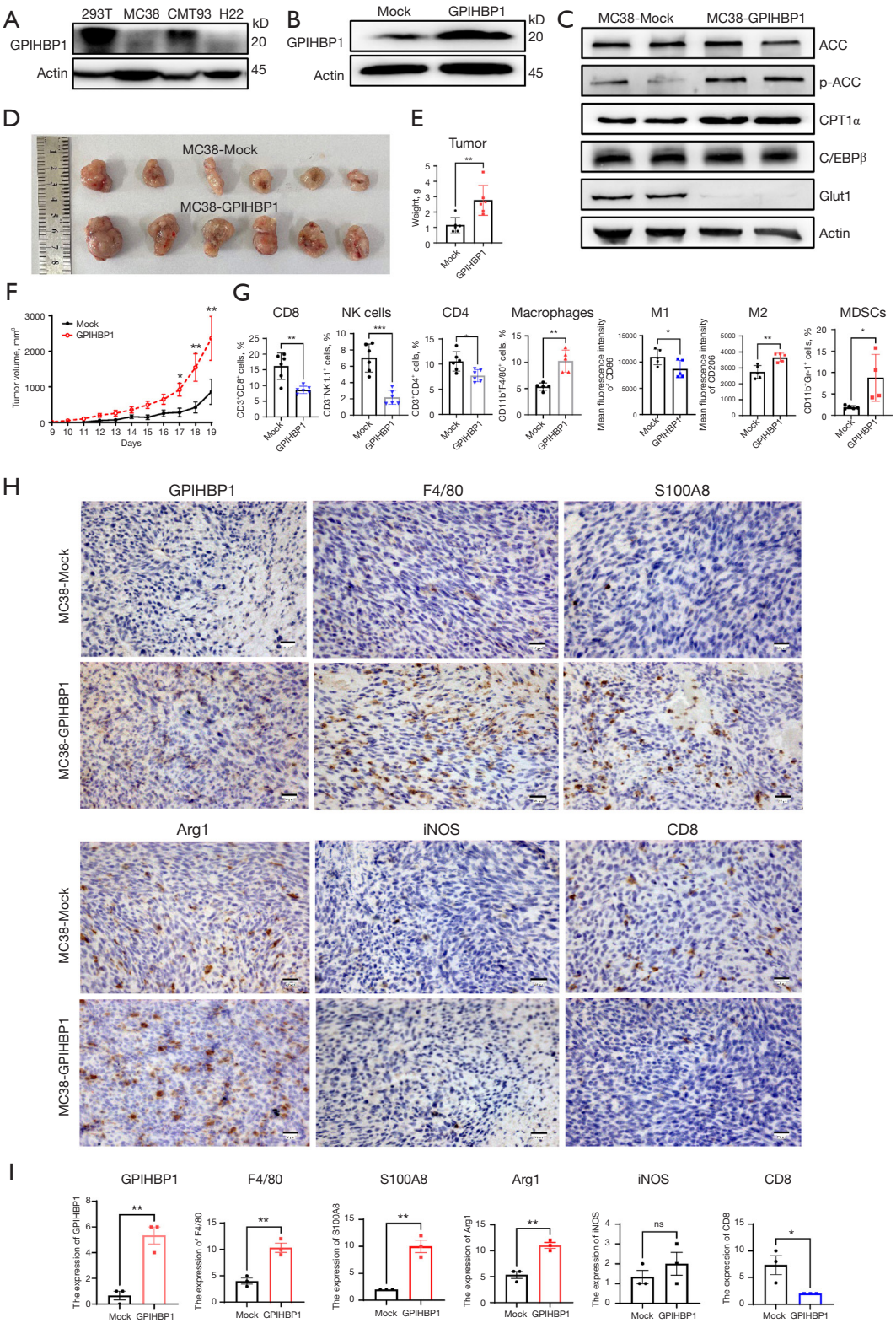

Figure 5 Ectopic expression of GPIHBP1 promoted tumour growth and immune evasion *in vivo*. (A) Expression of GPIHBP1 in 293T, MC38, CMT93, and H22 cell lines identified by Western blot. (B) Overexpression of GPIHBP1 in MC38 cells. (C) Variations of key proteins in glycolipid metabolism between MC38-Mock and MC38-GPIHBP1. *In vivo* tumours formed by MC38-Mock or

MC38-GPIHBP1 cells (D,E) (n=6). (F) Growth curve of tumour in tumour-bearing mice. (G) Frequencies of infiltrating immune cells detected by flow cytometry, including $CD8^+$ T cells ($CD3^+CD8^+$), NK cells ($CD3^-NK1.1^+$), $CD4^+$ T cells ($CD3^+CD4^+$), Macrophages ($CD11b^+F4/80^+$), M1 ($CD11b^+F4/80^+CD86^+$), M2 ($CD11b^+F4/80^+CD206^+$) and MDSCs ($CD11b^+Gr\text{-}1^+$). Representative IHC staining results of GPIHBP1, F4/80, S100A8, Arg1, iNOS, and CD8 (scale bar: 20 μm) (H) and respective statistics (I). The experiment was repeated twice. ns, no significance; *, P <0.05; **, P<0.01; ***, P<0.001. GPIHBP1, GPI-anchored high-density lipoprotein-binding protein 1; GPI, glycosylphosphatidylinositol; NK, natural killer; MDSC, myeloid-derived suppressor cell; Arg1, arginase 1; iNOS, inducible nitric oxide synthase; IHC, immunohistochemistry.

In summary, the results may suggest that the high GPIHBP1 expression in tumour cells facilitated immune evasion.

Discussion

As a key metabolic molecule, the involvement of GPIHBP1 in CRC progression is still unknown. Here, we demonstrated that GPIHBP1 expression in carcinoma cells decreased at the early stage of CRC but increased at the late stage. However, the GPIHBP1 expression of stromal cells gradually increased with CRC progression. Additionally, the high GPIHBP1 expression indicated poor immune surveillance as demonstrated by the abundant presence of tumour-promoting myeloid cells and the scarcity of tumour-inhibiting lymphocytes (such as $CD8^+$ T and NK cells) within the tumour tissues. This study firstly presented that tumour cells themselves could upregulate GPIHBP1 expression to facilitate immune evasion.

GPIHBP1 is mainly expressed in capillary endothelial cells (23). We revealed that GPIHBP1 could be induced in transformed tumour cells, particularly in metastatic tumour cells. In the early stage of CRC, the decreased GPIHBP1 expression in carcinoma cells is consistent with the rapid proliferation of tumour cells that rely on anaerobic glycolysis for energy (24). Tumour invasion and metastasis occur in advanced CRC. The up-regulated expression of GPIHBP1 indicated that tumour cells need effective energy supply (such as fatty acid oxidation) for migration (25). The molecular mechanisms of GPIHBP1 induction in the late stage of CRC cells possibly involve hypoxia, TGF-β or other factors in the tumour microenvironment (26,27).

The presence of many tumour-promoting myeloid cells and few tumour-inhibiting lymphocytes in the advanced stage CRC and MC38-GPIHBP1-transplanted tumours confirmed that the GPIHBP1 level in tumour cells affected the shape of tumour immune microenvironment (28). However, how GPIHBP1 in tumour cells influence the recruitment of immune cells warrants study. Given that the stromal cells of CRC samples were positively stained by the antibody against GPIHBP1, GPIHBP1 was speculated to be present in interstitial immune cells.

Admittedly, there were several limitations in this study. Firstly, we utilized the GPIHBP1 overexpression tumour-bearing mouse model to examine the association between GPIHBP1 expression and immune cell infiltration and tumour progression. However, in order to confirm the significant mechanisms, further studies using GPIHBP1 knockout cell or mouse lines are required. Secondly, we solely relied on public databases to demonstrate that there were no significant differences in GPIHBP1 expression between M0 and M1 tumours. Additional *in vivo/vitro* studies are needed to validate the metastasis characteristics. Lastly, the promotion of tumour growth by GPIHBP1 overexpression contradicts the clinical data, which indicated decreased GPIHBP1 expression in tumorous tissues compared to non-tumorous counterparts. Therefore, a more comprehensive investigation is needed to determine the precise effect of GPIHBP1 in both early and late stages of tumorigenesis.

Conclusions

The increased GPIHBP1 expression in advanced CRC is beneficial to self-invasion and metastasis, and reshapes the local immune microenvironment. Suppression of GPIHBP1 expression would theoretically repress the progression of CRC in patients with advanced CRC.

Acknowledgments

Funding: This work was supported by the National Natural Science Foundation of China (Nos. 82272809, 82102901, 81873866, and 81873867) and the Social Development Foundation of Jiangsu Province, China (No. BE2022775).

Footnote

Reporting Checklist: The authors have completed the

ARRIVE reporting checklist. Available at https://tcr.amegroups.com/article/view/10.21037/tcr-23-1766/rc

Data Sharing Statement: Available at https://tcr.amegroups.com/article/view/10.21037/tcr-23-1766/dss

Peer Review File: Available at https://tcr.amegroups.com/article/view/10.21037/tcr-23-1766/prf

Conflicts of Interest: All authors have completed the ICMJE uniform disclosure form (available at https://tcr.amegroups.com/article/view/10.21037/tcr-23-1766/coif). The authors have no conflicts of interest to declare.

Ethical Statement: The authors are accountable for all aspects of the work in ensuring that questions related to the accuracy or integrity of any part of the work are appropriately investigated and resolved. The study was conducted in accordance with the Declaration of Helsinki (as revised in 2013). This research involving human participants was reviewed and approved by the Ethics Committee of the Affiliated Hospital of Yangzhou University (No. 2021-YKL4-28-004). All patients signed informed consent forms. The animal study was reviewed and approved by the Institutional Animal Care and Use Committee of Yangzhou University (No. YXYLL-2022-56), Yangzhou, China, in compliance with institutional guidelines for the care and use of animals.

References

1. Fong LG, Young SG, Beigneux AP, et al. GPIHBP1 and Plasma Triglyceride Metabolism. Trends Endocrinol Metab 2016;27:455-69.
2. Young SG, Fong LG, Beigneux AP, et al. GPIHBP1 and Lipoprotein Lipase, Partners in Plasma Triglyceride Metabolism. Cell Metab 2019;30:51-65.
3. Weinstein MM, Yin L, Beigneux AP, et al. Abnormal patterns of lipoprotein lipase release into the plasma in GPIHBP1-deficient mice. J Biol Chem 2008;283:34511-8.
4. Beigneux AP, Miyashita K, Ploug M, et al. Autoantibodies against GPIHBP1 as a Cause of Hypertriglyceridemia. N Engl J Med 2017;376:1647-58.
5. Kurooka N, Eguchi J, Wada J. Role of glycosylphosphatidylinositol-anchored high-density lipoprotein binding protein 1 in hypertriglyceridemia and diabetes. J Diabetes Investig 2023;14:1148-56.
6. Bian X, Liu R, Meng Y, et al. Lipid metabolism and cancer. J Exp Med 2021;218:e20201606.
7. Martínez-Reyes I, Chandel NS. Cancer metabolism: looking forward. Nat Rev Cancer 2021;21:669-80.
8. La Vecchia S, Sebastián C. Metabolic pathways regulating colorectal cancer initiation and progression. Semin Cell Dev Biol 2020;98:63-70.
9. Zanotelli MR, Zhang J, Reinhart-King CA. Mechanoresponsive metabolism in cancer cell migration and metastasis. Cell Metab 2021;33:1307-21.
10. Ghanavat M, Shahrouzian M, Deris Zayeri Z, et al. Digging deeper through glucose metabolism and its regulators in cancer and metastasis. Life Sci 2021;264:118603.
11. Yang L, Venneti S, Nagrath D. Glutaminolysis: A Hallmark of Cancer Metabolism. Annu Rev Biomed Eng 2017;19:163-94.
12. Bergers G, Fendt SM. The metabolism of cancer cells during metastasis. Nat Rev Cancer 2021;21:162-80.
13. Li M, Xian HC, Tang YJ, et al. Fatty acid oxidation: driver of lymph node metastasis. Cancer Cell Int 2021;21:339.
14. Ruan C, Meng Y, Song H. CD36: an emerging therapeutic target for cancer and its molecular mechanisms. J Cancer Res Clin Oncol 2022;148:1551-8.
15. Park JK, Coffey NJ, Limoges A, et al. The Heterogeneity of Lipid Metabolism in Cancer. Adv Exp Med Biol 2021;1311:39-56.
16. Hashim NAA, Ab-Rahim S, Suddin LS, et al. Global serum metabolomics profiling of colorectal cancer. Mol Clin Oncol 2019;11:3-14.
17. The Cancer Genome Atlas. Colon and Rectal Cancer. 2023. Available online: https://portal.gdc.cancer.gov
18. Bindea G, Mlecnik B, Tosolini M, et al. Spatiotemporal dynamics of intratumoral immune cells reveal the immune landscape in human cancer. Immunity 2013;39:782-95.
19. Hänzelmann S, Castelo R, Guinney J. GSVA: gene set variation analysis for microarray and RNA-seq data. BMC Bioinformatics 2013;14:7.
20. Locati M, Curtale G, Mantovani A. Diversity,

Mechanisms, and Significance of Macrophage Plasticity. Annu Rev Pathol 2020;15:123-47.
21. Veglia F, Sanseviero E, Gabrilovich DI. Myeloid-derived suppressor cells in the era of increasing myeloid cell diversity. Nat Rev Immunol 2021;21:485-98.
22. Tan YS, Lei YL. Isolation of Tumor-Infiltrating Lymphocytes by Ficoll-Paque Density Gradient Centrifugation. Methods Mol Biol 2019;1960:93-9.
23. Young SG, Song W, Yang Y, et al. A protein of capillary endothelial cells, GPIHBP1, is crucial for plasma triglyceride metabolism. Proc Natl Acad Sci U S A 2022;119:e2211136119.
24. Ghashghaeinia M, Köberle M, Mrowietz U, et al. Proliferating tumor cells mimick glucose metabolism of mature human erythrocytes. Cell Cycle 2019;18:1316-34.
25. Andrzejewski S, Klimcakova E, Johnson RM, et al. PGC-1α Promotes Breast Cancer Metastasis and Confers Bioenergetic Flexibility against Metabolic Drugs. Cell Metab 2017;26:778-87.e5.
26. Miska J, Lee-Chang C, Rashidi A, et al. HIF-1α Is a Metabolic Switch Between Glycolytic-Driven Migration and Oxidative Phosphorylation-Driven Immunosuppression of Tregs in Glioblastoma. Cell Rep 2022;39:110934. Erratum for: Cell Rep 2019;27:226-37.e4.
27. Xie F, Ling L, van Dam H, et al. TGF-β signaling in cancer metastasis. Acta Biochim Biophys Sin (Shanghai) 2018;50:121-32.
28. Cassim S, Pouyssegur J. Tumor Microenvironment: A Metabolic Player that Shapes the Immune Response. Int J Mol Sci 2019;21:157.

Cite this article as: Gao M, Liao L, Lin Z, Hu X, Jia L, Gong W, Jia X. Increase in GPIHBP1 expression in advanced stage colorectal cancer indicates poor immune surveillance. Transl Cancer Res 2024;13(6):2691-2703. doi: 10.21037/tcr-23-1766

